Paper 83

Proceedings of the Eighth International Conference
on Engineering Computational Technology,
B.H.V. Topping, (Editor),
Civil-Comp Press, Stirlingshire, Scotland

Simulation and Validation of Valve Springs in Valve Train Simulations

J. Clauberg, B. Huber and H. Ulbrich
Department of Mechanical Engineering
Institute of Applied Mechanics
Technical University of Munich, Germany

Abstract

In the first part of this paper an overview of smooth and non-smooth multibody dynamics is given and numerical simulation tequniques for non-smooth multibody systems with impacts are considered. The second part deals with valve springs and different existing valve spring models. A new valve spring model, based on the approximation of the spring as a curved beam, is presented and validated using a test rig. The paper concludes with the integration of the new developed and implemented valve spring model in a complete valve train simulation. The application example allows to compare between the new valve spring model and a multi-mass model regarding to computational time using different integrators with smooth and non-smooth contact mechanics.

Keywords: valve spring, valve train simulation, multibody dynamics, nonsmooth dynamics, contact modelling, numerical integration.

1 Introduction

An important aim in todays combustion-engine-design is the reduction of fuel consumption and emission. Therefore small engines (downsizing) with low internal friction and raised power densitiy are employed.
This results in an increase of requirements on the valve train, which controls the charge changing. Charge changing denotes the cyclical process where the exhaust gases are exchanged with the fresh air fuel mixture. This exchange is done by cyclically lifting and closing the valves according to the contour of the camshaft. Valve springs press the valves into their seats when the valves are closed and against the camshaft contour when the valves are lifted.
In conventional valve trains the valve springs are the most flexible components. Hence,

the valve springs are answerable for the lowest resonance frequency, which significantly influences the dynamic behaviour of the valve train. The internal dynamics of the valve spring itself is mainly influenced by the moving masses of the coils and the contacts between the windings, which lead to a nonlinear spring characteristic.

Against the background of reducing development time and effort for combustion engines, increasingly simulation methods like multi-body-simulation are used. The main advantage of simulation methods is the fast and cheap calculation of different system configurations. Especially, if the development of valve trains with fully variable valve lift and valve timing is considered, where a lot of different system configurations have to be investigated, the advantage of simulation against experiment is obvious.
In order to achieve meaningful results in valve train simulations, detailed models of all components are necessary. As already mentioned above, especially the valve spring is dominant in the valve train dynamics. Thus, the implemented valve spring model has to be able to represent the dynamic effects of the real valve spring.

The first part of the paper deals with numerical aspects of multi-body-simulations, especially focussing on smooth- and nonsmooth contact mechanics and special integration schemes for non-smooth multibody systems with impacts. In the second part an overview of valve springs is given and existing valve spring models are described. A new valve spring model, based on a curved beam, is presented. The aim of this model is to comprise the simulation of different spring forms, the effects of the moving masses of the coils and contacts between the windings and to allow for reasonable computational times within a multi-body simulation. Using a test rig the valve spring model is validated in the static and the dynamic case. In the last part of the paper the presented valve spring model is integrated in a complete valve train and its advantages compared to a multi-mass spring model are shown using different integration methods with smooth and nonsmooth contact mechanics.

2 Multibody Dynamics

In this section a brief overview of multibody dynamics is given from the numerical point of view.

The first subsection deals with the equations of motion describing smooth- and non-smooth multibody systems. The second subsection addresses single-valued and set-valued force laws, that are used within the simulation models proposed in this paper. The last subsection shortly describes the computational environment for the presented methods and models.

2.1 Equations of Motion

The dynamical behaviour of a single-valued uni- and bilateral constrained multibody system can be described by the well known Equation (1) [1].

$$
\begin{aligned}
\mathbf{M}(\vec{q})\dot{\vec{u}} &= \vec{h}(\vec{u},\vec{q},t) \\
\dot{\vec{q}} &= \mathbf{T}(\vec{q})\vec{u}
\end{aligned} \tag{1}
$$

The system state is defined by the generalized positions $\vec{q}$ and the generalized velocities $\vec{u}$. The linear relationship between the generalized positions and generalized velocities is expressed by the kinematic matrix $\mathbf{T}(\vec{q})$ that is depending on the generalized positions $\vec{q}$. In the case of spatial motion the angular velocities are not integrable. The matrix $\mathbf{T}$ offers the possibility to use different parameters for $\vec{q}$ and $\vec{u}$. The vector $\vec{h}$ contains all single-valued external, internal and gyroscopic forces depending on the generalized positions $\vec{q}$, generalized velocities $\vec{u}$ and the time t.

Equation (1) relates accelerations to forces and is therefore not suitable to model non-smooth multibody systems with impacts. To describe non-smooth uni- and bilateral constrained multibody systems with impacts Equation (1) is replaced by the *Measure Differential Equation* (2) [2].

$$
\begin{aligned}
\mathbf{M}(\vec{q})d\dot{\vec{u}} &= \vec{h}(\vec{u},\vec{q},t)dt + \mathbf{W}(\vec{q})d\vec{\Lambda} && \text{(2a)} \\
\dot{\vec{q}} &= \mathbf{T}(\vec{q})\vec{u} && \text{(2b)} \\
(\vec{\Lambda},\vec{u},\vec{q},t) &\in \mathcal{N}
\end{aligned}
$$

$\vec{\Lambda}$ describes the impulses of the set-valued force laws and the matrix $\mathbf{W}(\vec{q})$ depending on the generalized positions $\vec{q}$ describes their projections. The acceleration measure $d\dot{\vec{u}}$ can be divided in a Lebesgue-continuous part $\dot{\vec{u}}dt$ and an atomic part $(\vec{u}^+ - \vec{u}^-)\,d\eta$ (left and right limit $\vec{u}^-$, $\vec{u}^+$) with the Dirac point measure $d\eta$. Similarly, the measure for impulses can be divided into a Lebesgue-continuous part $\vec{\lambda}dt$ and an atomic part $\vec{\Lambda}d\eta$. Taking the *Dirac* [1] delta function into account, Equation (2) can be integrated resulting in Equation (3).

$$
\begin{aligned}
\mathbf{M}(\vec{q})\dot{\vec{u}} &= \vec{h}(\vec{u},\vec{q},t) + \mathbf{W}(\vec{q})\vec{\lambda} && \text{(3a)} \\
\mathbf{M}_i\left(\vec{u}_i^+ - \vec{u}_i^-\right) &= \mathbf{W}_i\,\vec{\Lambda}_i \qquad \forall i \in N && \text{(3b)} \\
\dot{\vec{q}} &= \mathbf{T}(\vec{q})\vec{u} \\
(\vec{\Lambda},\vec{\lambda},\vec{u},\vec{q},t) &\in \mathcal{N}
\end{aligned}
$$

Equation (3a) is valid for smooth parts of the time integration and Equation (3b) is valid at all times t_i of impact.

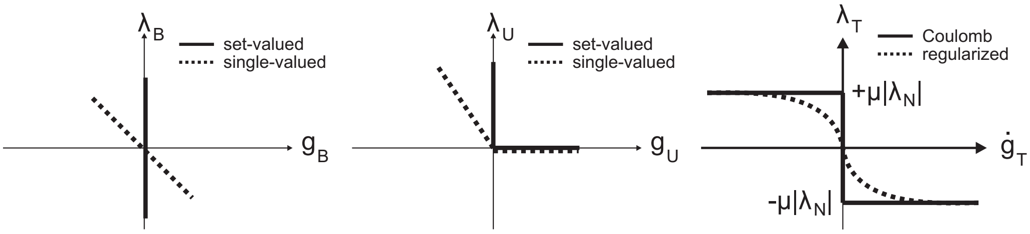

(a) Bilateral constraint (b) Unilateral constraint (c) Planar *Coulomb* friction

Figure 1: Force laws for bi- and unilateral contacts and friction

2.2 Single- and Set-Valued Force Laws

Force laws within multibody dynamics can be mainly divided into single- and set-valued force laws. Single-valued force laws depend on the system state $(\vec{q}, \vec{u}, t)$ and are explicitly evaluated. Set-valued force laws are only depending implicitly on the system state $((\vec{\Lambda}, \vec{\lambda}, \vec{u}, \vec{q}, t) \in \mathcal{N})$ and therefore have to be solved by special numerical methods. Mainly two different methods have been approved to be suitable: the formulation as *Linear Complementarity Problems* and the formulation with the *Proximal Point to a Convex Set* [2], a method from the convex analysis. In this paper, the *Proximal Point to a Convex Set* is used for solving the set-valued force laws.

Uni- and bilateral set-valued force laws can be seen as spring-damper combinations with infinite stiffness. They have the advantage that uni- and bilateral constraints can be modelled in a physically motivated way and that they do not need uncertain parameters like spring-stiffnesses or spring-dampings. Furthermore, set-valued friction laws allow to model stick-slip effects within frictional contacts.

In multibody dynamics, basically three types of set-valued force laws are needed: bilateral constraints (Figure 1(a)), unilateral constraints (Figure 1(b)) and friction (Figure 1(c)).

A bilateral constraint can be interpreted as a bilateral force law (e.g. joints) of the form

$$g_B = 0, \qquad \lambda_B \in \mathbb{R}\,, \tag{4}$$

a unilateral constraint can be interpreted as a unilateral force (e.g. contacts) which are given by the *Signorini-Fichera*-condition

$$g_U \geq 0, \quad \lambda_U \geq 0, \quad g_U\,\lambda_U = 0 \tag{5}$$

with $g_{B,U}$ the normal distance between two bodies and $\vec{\lambda}_{B,U}$ the corresponding forces.

Friction is modelled by *Coulomb* friction that can be mathematically described by

$$\begin{array}{llll} \dot{\vec{g}}_T = \vec{0} & \Rightarrow & \left|\vec{\lambda}_T\right| & \leq \mu\;|\lambda_N| \\ \dot{\vec{g}}_T \neq \vec{0} & \Rightarrow & \vec{\lambda}_T & = -\frac{\dot{\vec{g}}_T}{\left|\dot{\vec{g}}_T\right|}\,\mu\;|\lambda_N|\;, \end{array} \tag{6}$$

with $\dot{\vec{g}}_T$ the tangential velocities, μ the friction coefficient, λ_N the normal and $\vec{\lambda}_T$ the tangential forces.

2.3 Integration Schemes

There are essentially two classes of integration schemes suitable for non-smooth multibody systems with impacts, namely *Event Driven Integration Schemes* and *Time Stepping Integration Schemes*. In this paper two different time stepping integration schemes are used: a half-explicit time-stepping scheme with constant time step size and a "state of the art" time-stepping integration scheme with step size adjustment and parallelization within the integrator [3]. Both integration schemes are formulated on velocity level leading to the advantage that the continuous and discontinuous dynamic can be treated in the same way.

2.3.1 Half-Explicit Time-Stepping Integration Scheme

It isn't the aim of this paper to explain time-stepping integration schemes in detail, therefore only the two main discretization steps will be outlined. The discretization of Equation (2b) leads to

$$\int_{t^l}^{t^{l+1}} \mathbf{T}\vec{u}dt \approx \mathbf{T}^l\vec{u}^l\Delta t^l \tag{7}$$

and the discretization of Equation (2a) leads to

$$\int_{t^l}^{t^{l+1}} \mathbf{M}^{-1}(\vec{h}dt + \mathbf{W}d\vec{\Lambda}) \approx (\mathbf{M}^{l+1})^{-1}(\tilde{\vec{h}}^{l+1}\Delta t + \mathbf{W}_a^{l+1}\vec{\Lambda}_a^{l+1}) \tag{8}$$

with l denoting the current and $l+1$ the next time step and $\tilde{\vec{h}}^{l+1} = \vec{h}(\vec{u}^l, \vec{q}^{l+1}, t^{l+1})$. More information about the half-explicit time-stepping integration scheme with constant time step size can be found in FOERG [2].

2.3.2 Time Stepping Integration Scheme with Step Size Adjustment

The main drawback of the time stepping integration scheme of Sec. 2.3.1 is the missing step size adjustment. In HUBER [3], the focus is on time stepping integration schemes with higher order and step size adjustment. In this paper we use his "state of the art" integration scheme with step size selection based on *Richardson* extrapolation and parallelization within the integrator.

2.4 Computational Environment

All models are implemented and simulated in the multibody simulation environment MBSim [4]. MBSim has been developed at the Institute of Applied Mechanics (Technische Universität München) and is available under the GNU Lesser General Public

License. It is written in C++ and provides a simulation framework for dynamic systems of various physical domains (eg. multibody dynamics, hydraulics, electronics, control theory) as well as post-processing tools (OpenMBV for system visualization [5], h5plotserie for data visualization [6]).

3 Valve Spring Model

In the first part of this section the most important characteristics of valve springs are investigated, commonly used forms of valve springs are introduced and an overview on dynamic valve spring models is given.
In the second part a new continuous valve spring model based on the approximation of the spring winding as a curved beam is presented.

3.1 Valve Springs and Valve Spring Models

The main purpose of valve springs as part of the valve train is the controlled closing of the valves by sustaining the force closure between the valve train components during the valve movement. On the one hand the spring force has to be high enough to prevent the valve from bouncing of the seating when closing the valve and to prevent the valve from lifting of the camshaft when opening the valve. Taking the aim of low frictional losses into account to reduce the fuel consumption of combustion-engines on the other hand, low spring forces should be aspired.

To avoid excessive vibrations at high rotational speeds of the engine, today most valve springs have a *progressive behaviour*, which denotes an increasing spring rate and resonance frequency of the valve spring with increasing deflection. The progressive behaviour is achieved by a non-constant pitch between adjacent coils. Depending on the winding-geometry of the spring this causes some coils come into contact earlier than other coils. The more the spring is compressed the more coils come into contact and are excluded from the elastic deformation of the spring, which results in higher spring stiffnesses.
If the operating frequency is close to the resonance frequency of the valve spring a phenomenon called *surging* occures. The consequences are high stresses and forces, which have negative effects on the durability of the spring and cause an erratically opening or closing of the valve. If the forces and the resulting vibrations are high enough, the coils can even impact one another, which is called *coil clash*.

3.1.1 Common Valve Spring Forms

Mainly four different forms of valve springs, which are depicted in Figure 2, are used currently [7]. With a constant coil diameter and symmetric coil distances the *cylindrical symmetric* valve spring is the standard form. The main characteristic of the *cylindrical asymmetric* spring are smaller coil distances at the sides close to the cylinder head, which implies less moved masses. Usage of *conical* springs allows a small compressed length and small moved masses but generally a less progressive behaviour is expected. Finally *beehive* valve springs combine small moved masses (upper conical part) with progressive behaviour (lower cylindrical part).

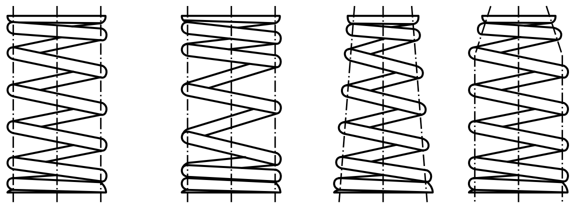

Figure 2: Common valve spring forms

3.1.2 Dynamic Valve Spring Models

In valve train simulations mainly three different dynamic spring models are implemented.
The *modal model* is based on the theory of modal analysis, which allows the description of the motion of a flexible body as a superposition of its weighted eigenmodes. Often it is sufficient to consider only the first few eigenmodes, which means a low number of degrees of freedom and therefore relatively small computational times. The main disadvantage of this model is, that the contact between coils cannot be modeled and thus makes the modal model unfeasible for detailed valve train simulations. A reduced modal model is presented by PHILIPS ET. AL. in [8] and the extension of this model for nonlinear valve springs is shown by SCHAMEL ET. AL. in [9].
Using the *multi mass model* the valve spring is described by a series of discrete masses coupled with spring-damper-elements. In his work [10] ENGELHARDT proposes the discretization of each coil by four to eight masses for good results, leading to a high number of degrees of freedom of the model. Another drawback is, that mostly the equations of motion become numerically stiff using the multi mass model, which causes numerical problems and high computatonal times. The advantages are that contacts between the coils and the progressive behaviour of the spring can be modeled.
A different approach is pursued by the *multi beam model*. Here the spring is approximated by a discrete number of straight beams arranged in series. For good approximations of the curved spring geometry with straight beams, a large number of beam elements is needed, leading to a high numer of degrees of freedom of the model. TICHANEK ET. AL. [11] for example uses 24 beam elements per coil. The multi beam model also allows for the modelling of coil contacts and the progressive behaviour.

3.2 Valve Spring Model based on Curved Beam

Following the aim of delivering a valve spring model with few degrees of freedom that allows contact modelling between the coils, representation of progressive nonlinear spring behaviour and produces less stiff equations of motion than the multi mass model, HUBER ET. AL. [12] proposed a curved beam model.
This model is picked up here and extended to the most common spring forms. As the derivation of the spring model can be looked up in detail in [12], here only the main steps and the accomplished extensions are described.

3.2.1 Equations of Motion

Starting point is the description of the kinematics of the spring, which is based on the approximation of the spring winding as a curved beam. By describing the motion of an arbitrary spring cross section, a relationship between the strains in the cross section and its translation, rotation and warping is gained.
The next step is the introduction of an isotropic hookean material law, which provides the relation between the strains and the stresses. By assuming an elliptical cross section of the spring the forces and moments acting on each point of the cross section can be estimated via integration of the stresses.
Finally, the equations of motion are obtained by applying the principles of linear and angular momentum on an infinitesimal beam-section. The resulting six coupled partial differential equations describe the translational and rotational motion of the spring.
As the spring model is intended to be used in valve train simulations, only the degree of freedom in direction of the spring axis is of interest. Assuming that the main part of the elastic energy of the spring results from the torsional deformation of the cross section, the reduced one-dimensional equation of motion for the spring can be derived according to Equation (9). This is a hyperbolic partial differential equation, which is also known as the one-dimensional wave equation.

$$\rho A \frac{d^2 u_z}{dt^2} - \frac{GJ}{R^2} \frac{d^2 u_z}{ds^2} = f_z \tag{9}$$

ρ denotes the density, A the cross section area, u_z the displacement in spring axis direction, t the time, G the shear modulus, J the torsional constant, R the radius, s the position on the spring wire and f_z the force in spring axis direction.

3.2.2 Discretization

To be able to integrate and use the spring model in a multi-body-simulation environment a discretization of Equation (9) is done by using the finite element approach. Therefore the Galerkin-Bubnov method is applied, resulting in the discretized equations of motion:

$$\underbrace{\int_k^l \rho A \vec{N}\vec{N}^T\, ds}_{\mathbf{M}} \cdot \frac{d^2\vec{q}}{dt^2} + \underbrace{\int_k^l \frac{GJ}{R^2}\frac{d\vec{N}}{ds}\frac{d\vec{N}^T}{ds}\, ds}_{\mathbf{K}} \cdot \vec{q} = \underbrace{\left[\vec{N}\cdot T_z\right]_k^l + \int_k^l \vec{N}\cdot f_z\, ds}_{\vec{F}} \qquad (10)$$

By choosing adequate form functions $\vec{N}$, with Equation (10) the constant mass-matrix $\mathbf{M}$, the constant stiffness-matrix $\mathbf{K}$ and the vector of the right hand side $\vec{F}$ for each element of the spring model can be calculated. As the spring radius is not constant for conical and beehive valve springs the radius R of each element of the spring model is approximated by the arithmetical mean value.
The implementation of the spring model provides four different element types, which are listed in Table 1. Besides the denotation of the elements Table 1 also contains the number of nodes and the degrees of freedom of each node.

Type of element	Number of nodes	Dofs per node
Lagrange 1. order	2	1
Lagrange 2. order	3	1
Lagrange 5. order	6	1
Cubic hermite	2	2

Table 1: Available elements in valve spring model implementation

3.2.3 Damping

As Equation (10) does not include any damping, a velocity-proportional damping term is added according to Equation (11).

$$\mathbf{M}\frac{d^2\vec{q}}{dt^2} + \mathbf{D}\frac{d\vec{q}}{dt} + \mathbf{K}\vec{q} = \vec{F}, \qquad \mathbf{D} = \mathbf{D}_1 + \mathbf{D}_2 + \mathbf{D}_3 \qquad (11)$$

The damping matrix includes material damping $\mathbf{D}_1$ (Equation (12)), discrete damping $\mathbf{D}_2$ (Equation (13)) and a damping amount $\mathbf{D}_3$ (Equation (14)), that takes energy losses due to rubbing coil windings into account. As the contacts open and close during the simulation, the damping Matrix $\mathbf{D}_3$ is calculated at every time step.

$$\mathbf{D}_1 = d_M \cdot \mathbf{M} + d_K \cdot \mathbf{K} \tag{12}$$

$$\mathbf{D}_2 = \begin{pmatrix} d_{dis} & \dots & 0 \\ \vdots & \ddots & \vdots \\ 0 & \dots & d_{dis} \end{pmatrix} \tag{13}$$

$$\mathbf{D}_3 = \begin{pmatrix} d_{cont} & 0 & \dots & \dots & \dots & 0 \\ 0 & \ddots & & & & \vdots \\ \vdots & & d_{cont} & & & \vdots \\ \vdots & & & 0 & & \vdots \\ \vdots & & & & \ddots & \vdots \\ 0 & \dots & & & \dots & 0 \end{pmatrix} \tag{14}$$

3.2.4 Contact Modelling

Simulation of springs with non-constant radius requires the adaption of the contact modeling. For this purpose spherical contact geometries are used. The radius k of the spheres is calculated taking into account on the one hand the non constant radius in combination with the elliptical cross section and the pitch on the other hand.

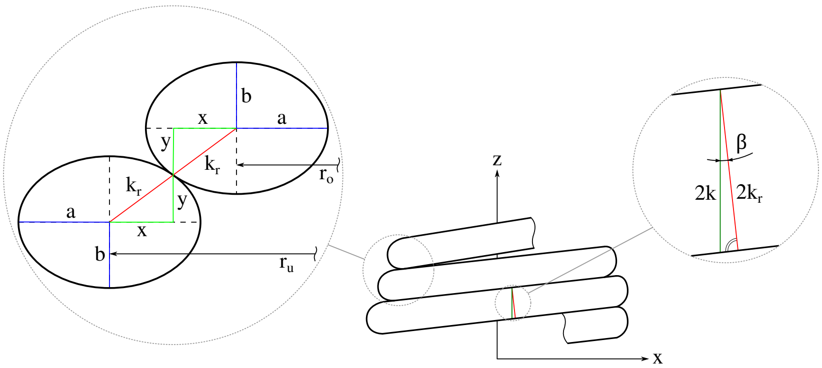

Figure 3: Geometrical Conditions in Closed Contact

The left part of Figure 3 shows the geometrical conditions in a contact of a spring with non-constant radius and an elliptical cross section. The radius k_r of the contact spheres for this configuration can be calculated according to Equations (15) to (17).

$$x = \frac{1}{2}(r_u - r_o) \tag{15}$$

$$y = b\sqrt{1 - \left(\frac{x}{a}\right)^2} \tag{16}$$

$$k_r = \sqrt{x^2 + y^2} \tag{17}$$

The effect of the pitch on the radius of the contact spheres is depicted in the right part of Figure 3. Assuming the pitch angle β to be constant in all closed contacts, the radius k is approximated according to Equations (18) and (19), where R_0 denotes the spring radius at the lower end.

$$\beta \approx \arctan\left(\frac{b}{\pi R_0}\right) \tag{18}$$

$$k \approx k_r \frac{1}{\cos\beta} \tag{19}$$

In the spring model an arbitrary number of contacts can be constituted. For each contact a contact sphere C_i and a target sphere T_i are positioned on the spring-wire. The first contact sphere is positioned on the lower end of the spring and the last contact sphere on the upper end. The remaining contacts are positioned equidistant in between. Figure 4 examplarily shows the positions of the contact and target spheres for a valve spring with five contacts.

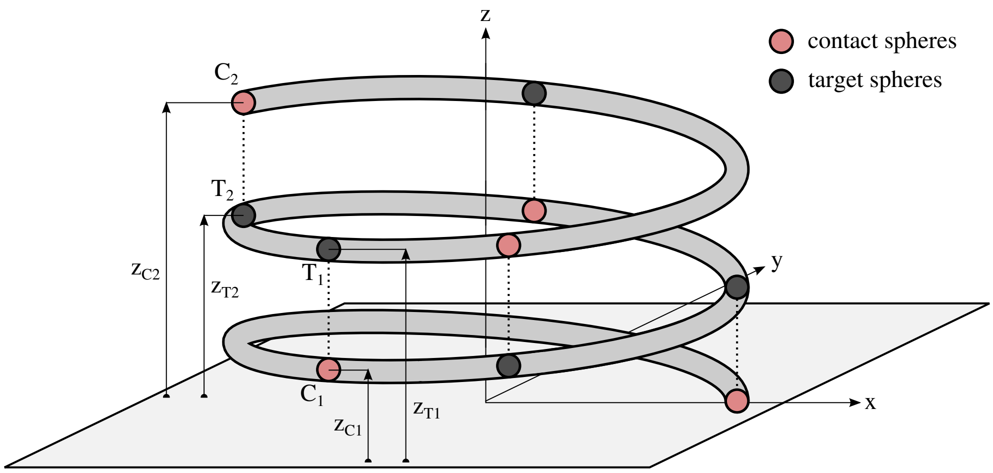

Figure 4: Contact Positions

4 Model Validation

In this section the validation of the spring model, presented in Section 3, with experimental data both in the static case and in the dynamic case is shown.

4.1 Examined Valve Springs

For the validation of the valve spring model three different, commercially available, valve springs are used, whose main characteristics are listed in Table 2. The material parameters (Youngs modulus E, lateral contraction coefficient ν, density ρ, shear modulus G) are provided by the manufacturers of the springs when available or set

Denotation	Form	Cross section	Windings	Vehicle
cyl	Cylindrical asymmetric	Elliptical	7	Audi
con	Conical	Elliptical	6	Audi A4
bee	Beehive	Elliptical	7	BMW 740Li

Table 2: Examined valve springs

in the standard range of spring materials. The geometrical parameters (geometry of the spring winding, cross section parameters) are determined using special measuring devices.

4.2 Static Validation

The static validation of the spring model is done using the load-deflection-diagram. In Figure 5 the experimental set-up is depicted. The valve spring is manually compressed with the handwheel and the current deflection and the spring force are measured using a laser and a force sensor.

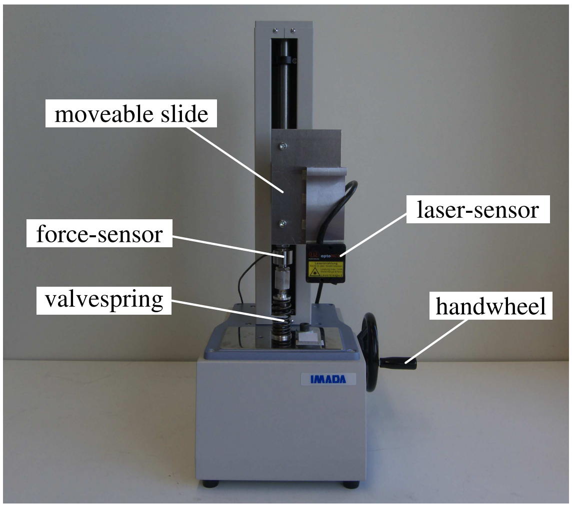

Figure 5: Experimental Set-Up for Measuring the Load-Deflection-Diagram

As listed in Table 3 for the simulation of the three valve springs seven cubic hermite elements are used. The spring “cyl” is modelled using seven and the other two springs using eight contacts. In Figure 6 the load-deflection-diagrams gained from the simulations are compared to the experimental data. It shows, that for all three springs the simulation represents the static nonlinear bahaviour of the real valve springs quite well. Especially the results for the springs “cyl” and “bee” are very good. The kinks in the simulated diagrams are a result of the discrete contact positions. Each time a contact is closed, the resulting stiffness of the spring increases and a kink occurs in the load-deflection-diagram. The little deviations when reaching block length are not

Spring	Element-type	Elements	Contacts
cyl	Cubic	7	7
con	Cubic	7	8
bee	Cubic	7	8

Table 3: Number of elements and contacts used for validation

really a drawback since they disappear with an increasing number of contacts and are practically irrelevant, if valve springs are not compressed up to block length.

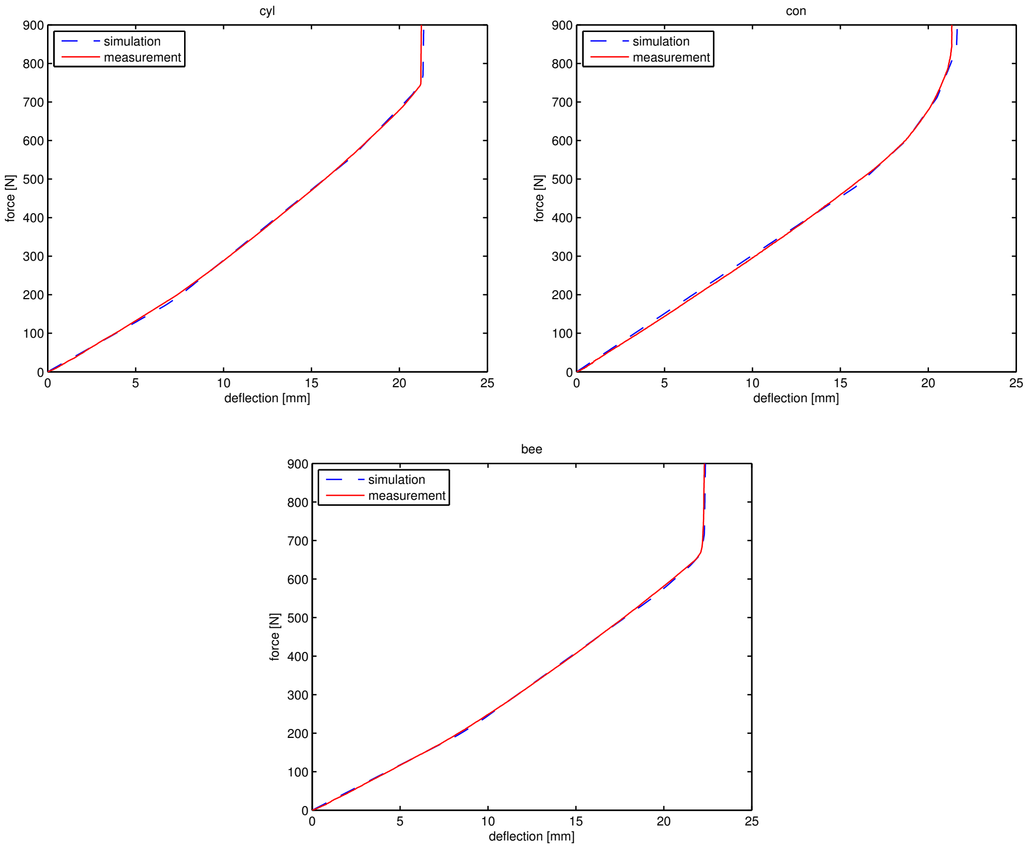

Figure 6: Load-Deflection-Diagrams of the Evaluated Valve Springs

4.3 Dynamic Validation

The dynamic validation is divided into the validation in the frequency domain, where the resonance frequencies are examined and into the validation in the time domain, where the time response of the spring to a dynamic excitation is investigated.
For the experiments the test rig depicted in Figure 7 is used. A electric motor drives the cam disc and the cam follower translates the contour of the cam disc to a translational

excitation on the valve spring. The spring force at the clamped end of the spring and the position of the excitating ram are measured by adequate sensors. By using different cam disc contours, variable spring excitations are realized. Here a cam disc creating a harmonic sinusoidal excitation with an amplitude of 0.005 mm (validation of the resonance frequencies) and a cam disc generating an excitation analog to the excitation created by the camshaft in a combustion engine (validation in the time domain) are used.
For simulations within the dynamic validation the same element-types and numbers of elements and contacts as within the static validation (see Table 3) are used.

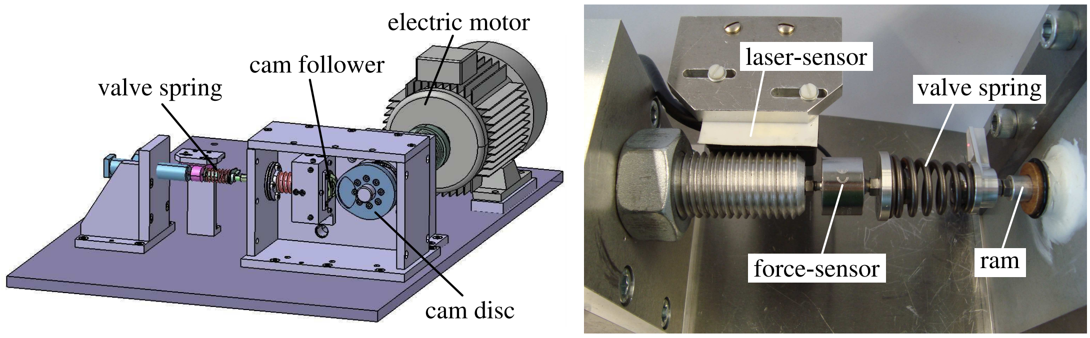

Figure 7: Test rig for dynamic validation

Frequency Domain

The resonance frequencies of the real spring are detected from a FFT-analysis of the force-signal of quasi-static run-up experiments in a frequency range of about 0 to 2000 Hz. Figure 8 exemplarily shows the frequency spectrum of the force at the lower end for the spring “bee” with a preload of 400 N. In the diagram the first three resonance frequencies are clearly depicted.

In Figure 9 the simulated and measured first two resonance frequencies of the three valve springs are compared for preloads between 50 and 625 N. The steps in the simulated frequency-curves – as the kinks in the simulated load-deflection-diagrams – are a consequence of the discrete contact positions. The resonance frequency of the spring model does only change, if the stiffness of the spring changes, i.e. when a contact is closed or opened. A comparison with Figure 6 shows, that the spring forces with a kink in the simulated load-deflection-diagrams are identical to the preloads with a step in the simulated frequencies in Figure 9.

Time Domain

For the validation of the spring model in the time domain, the measured ram position serves as excitation in the simulations. By applying a kalman-filter on the measured position-signal travel, velocity and acceleration of the excitation are prepared for the simulation.

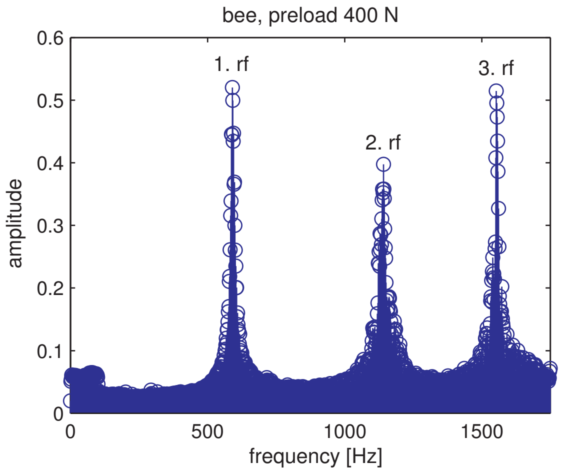

Figure 8: Frequency spectrum of force at lower spring end

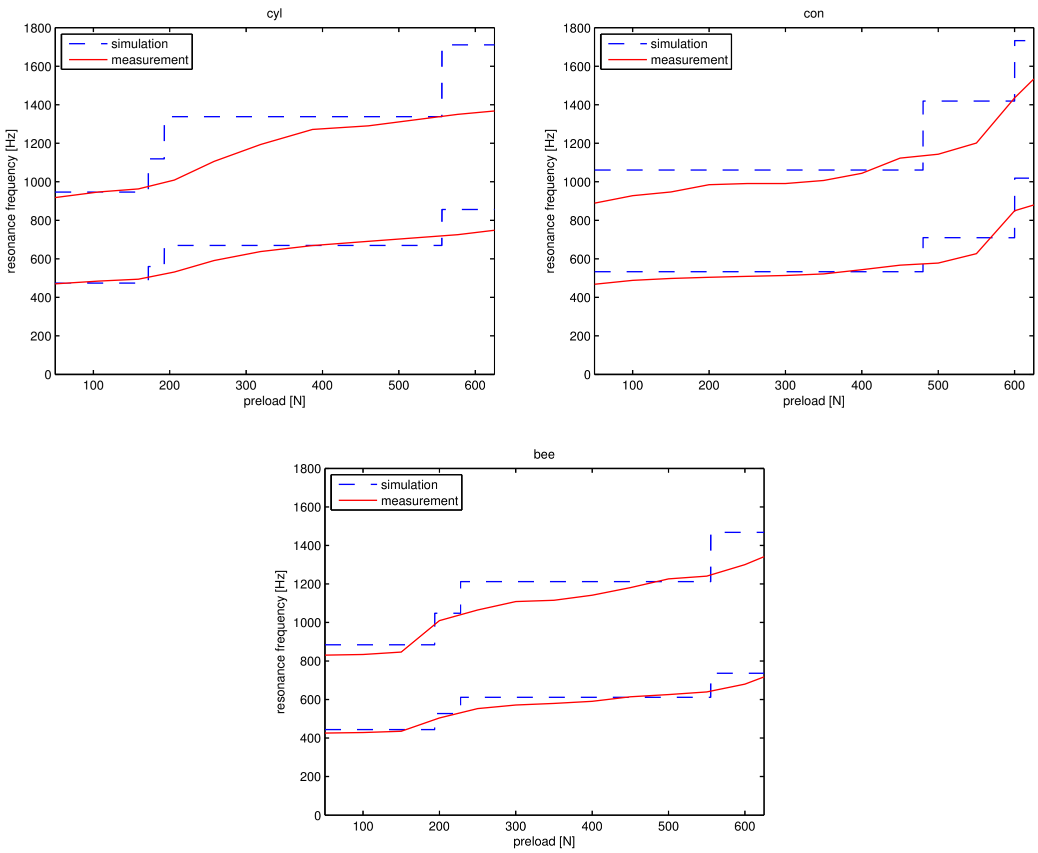

Figure 9: Resonance frequencies of the evaluated valve springs

Figure 10 depicts the simulated and measured forces at the clamped end of the three springs. The simulations reproduce the qualitative curves of the measurements quite well, but in some points deviations occur. In this context it has to be mentioned, that the damping parameters of the different damping terms explained in Section 3.2 have great influence on the simulation results. As the damping coefficients were adapted manually in this work, big potential is expected within the use of optimization methods for the damping-parameter identification.

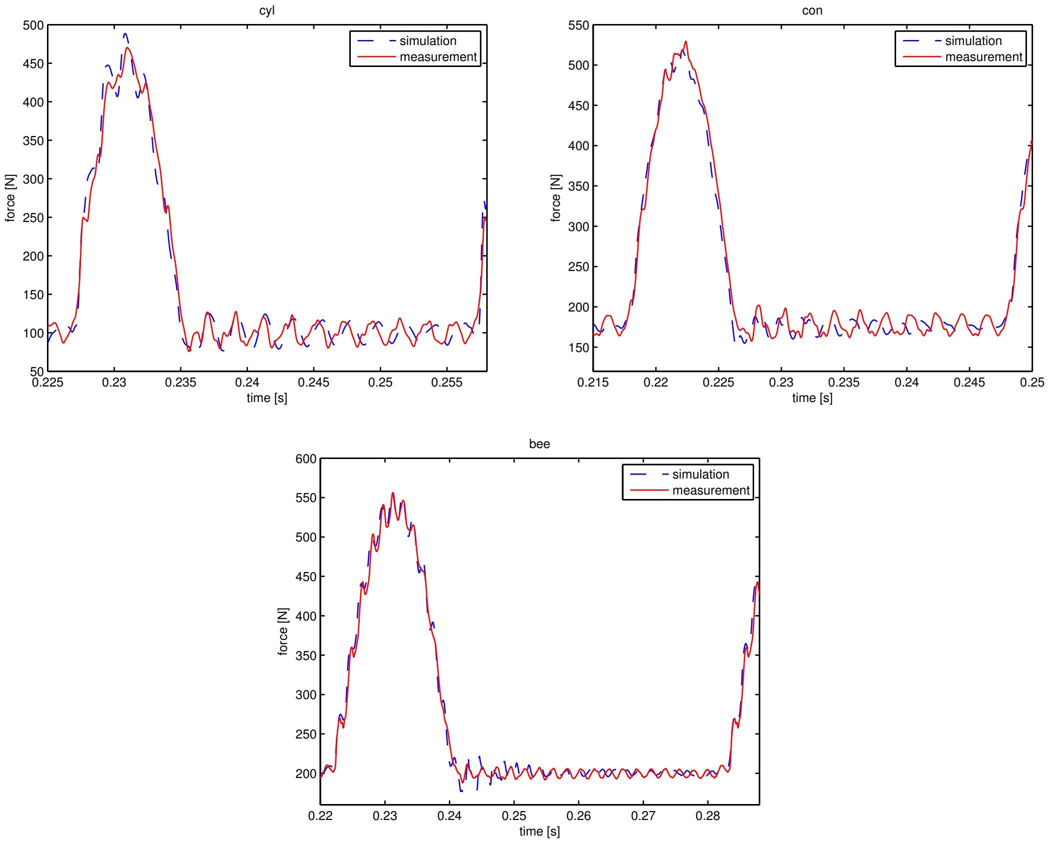

Figure 10: Force at clamped end of the evaluated valve springs

5 Valvetrain Model with Continuous Spring Model

To show the efficiency of the proposed continuous spring model, a valve train with twelve valve mechanisms is used (see Fig. 11). Each valve mechanism in Figure 11 [13] consists of the following parts: cam shaft, cam, roller, rockerarm, valvespring, valve and valveseat. Figure 11 also shows the mechanical contacts within each valve unit (contacts are written in white and bodies in black), their modeling is briefly outlined in Table 4.

Within this section we want to give some evidence that by using the proposed valve

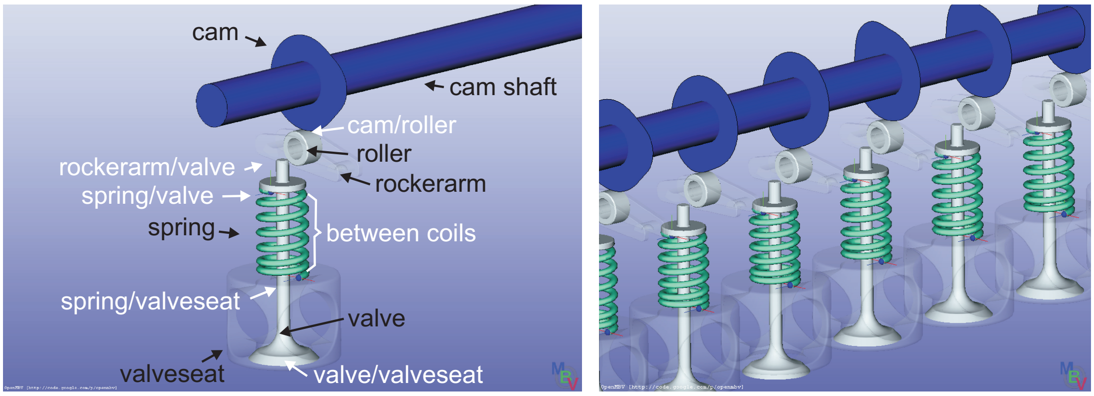

Figure 11: Valvetrain with continuous springs

Body 1	Body 2	Contour Pairing
cam	roller	spline contour to circle
rockerarm	valve	point to line
spring	valve	point to plane
spring	valveseat	point to plane
valve	valveseat	point to line

Table 4: Contacts within valve mechanism unit

spring model the equations of motion will get less numerically stiff (Subsection 5.1) than by using a common multi-mass model and we want to show some comparisons between smooth- and non-smooth multibody dynamics and the corresponding integration schemes regarding the necessary computational time.

5.1 Comparison to Multi-Mass-Model

The presented valve train is modeled in two ways. First using a common multi-mass model and second using the proposed continuous spring model with quadratic form functions. In order to compare these two models, it is necessary to decide how many degrees of freedom are needed to reach approximately the same accuracy. Therefore, the first two eigenfrequencies of the considered spring models are taken into account. Figure 12(a) shows the root-mean-square of deviation between the considered models and a detailed model in ANSys [12]. If the error has to be lower than approximately 0.6%, the multi-mass model needs about 20 degrees of freedom and the continuous spring model with quadratic form functions about 12 degrees of freedom. Due to this consideration, a multi-mass-model with 20 degrees of freedom and a continuous spring model with six quadratic elements are chosen. Both systems are integrated by a state of the art ODE integrator (LSODE) with step size adjustment and single-valued contact modeling. Figure 12(b) shows the normalized calculation times of the systems. It can be concluded that the continuous spring model with qudaratic form

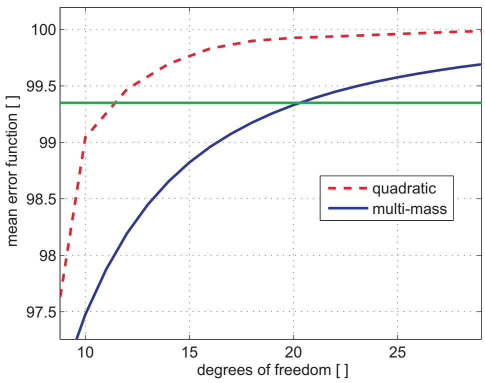

(a) Mean error function

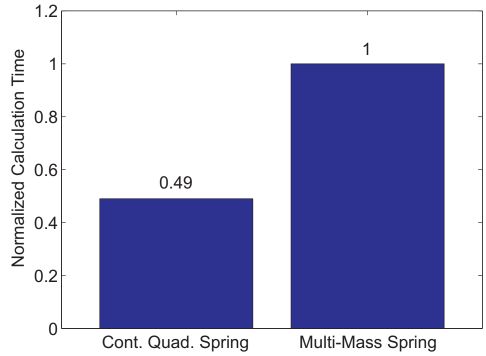

(b) Calculation times

Figure 12: Comparison between multi-mass and continuous spring model

functions is about 50% faster than the multi-mass-model, which can be explained by two reasons: the multi-mass model needs more degrees of freedom and the equations of motion are more numerically stiff (lower time step size needed).

5.2 Comparison of Smooth and Non-Smooth Contact Mechanics

In this section some comparsions between smooth and non-smooth contact mechanics and their corresponding integration schemes regarding the computational time are shown. Therefore, we use four different integration schemes: a common ODE integrator (LSODE), a half explicit time stepping integration scheme (see Subsection 2.3.1) and a time stepping integration scheme with step size adjustment (see Subsection 2.3.2) in its sequential and parallel version. Using time stepping integration schemes, contacts are modeled rigid (set-valued), using the LSODE integrator, contacts are modeled flexible (single-valued).

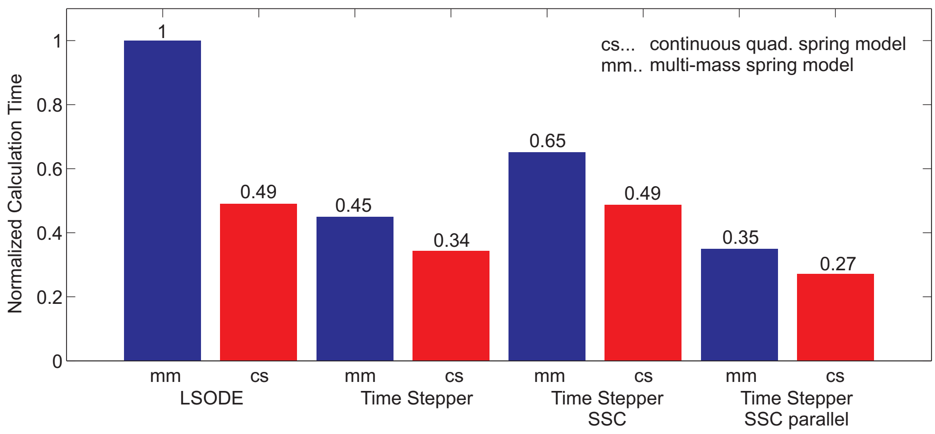

Figure 13: Comparison of calculation times

Figure 13 shows the results of the comparison. The continuous spring model (cs) with quadratic form functions is faster than the multi-mass model (mm) regardless of which integration scheme is used. Furthermore, rigid contact mechanics (set-valued force laws) lead to significantly lower computational times. The half-explicit time-stepping integration scheme (Time Stepper, cs) takes about 30% less computational time than the LSODE integrator (LSODE, cs). Even better results are obtained by using the parallel version of the time stepping integration scheme with step size adjustment (Time Stepper SSC parallel, cs). It is about 45% faster than the LSODE integrator (LSODE, cs). Setting the "stiff"-flag of the LSODE integrator leads to dramatically long simulation times and was therefore not considered further on. Similar results were obtained by FOERG [14]. In his comparison of smooth and non-smooth contact mechanics in valve trains without continuous springs.

6 Conclusion

The first part of the paper deals with smooth and non-smooth multibody dynamics. Therefore the equations of motion for non-smooth uni- and bilateral contraint systems with impacts are introduced. The constitutive laws governed by the set-valued force laws as well as special integration schemes for non-smooth mutlibody systems with impacts are described in the following sections.

In the second part, different aspects of valve springs are treated and commonly used valve spring models are described and compared regarding their suitability for multibody simulations of valve trains. A new valve spring model based on the approximation of the spring as a curved beam is presented. This approach leads to hyperbolic partial differential equations, which are discretized using the finite element method. The spring model is implemented and integrated in a multibody-simulation-environment and facilitates efficient simulations of the most common valve spring forms (cylindrical, conical, beehive). The main advantages of this model over the commonly used ones are fewer degrees of freedom together with contact modelling between the coils. The model adaptations, carried out for a commercially available cylindrical, a conical and a beehive valve spring, show great compliance between the simulations and measurements.

The third part shows the integration of the presented continuous spring model in a valve train comprising twelve valve unit mechanisms. Taking this example into account the efficiency of the proposed valve spring model is shown by comparing it to a common multi-mass spring model. It can be concluded that the continuous model is about 50% faster than the multi-mass model. To conclude the paper, smooth and non-smooth contact mechanics and their corresponding integration schemes are applied to the valve train. It shows that non-smooth contact mechanics is about 50% faster than smooth-contact mechanics for this application.

References

[1] F. Pfeiffer, ”Mechanical System Dynamics”, in ”Lecture Notes in Applied and Computational Mechanics”, Springer, Berlin, 2005.

[2] M. Förg, ”Mehrkörpersysteme mit mengenwertigen Kraftgesetzen - Theorie und Numerik”, Dissertation, Technische Universität München, 2008.

[3] R. Huber, H. Ulbrich, ”Integration of Non-Smooth Systems using Time-Stepping based Extrapolation Methods and DAE Solver Combined with Time-Stepping”, in ”Proceedings of the 2nd South-East European Conference on Computational Mechanics”, Rhodos, Greece, 2009.

[4] MBSim - Multi-Body Simulation Software. GNU Lesser General Public License, http://code.google.com/p/mbsim-env/

[5] OpenMP - Open Multi Body Viewer, http://code.google.com/p/openmbv/

[6] HDF5Serie - A HDF5 Wrapper for Time Series based on the hdf5 library, http://code.google.com/p/hdf5serie/

[7] R. Basshuysen, F. Schäfer, ”Handbuch Verbrennungsmotoren”, 5. Aufl. Wiesbaden, Vieweg + Teubner, GWV Fachverlag GmbH, 2010, ISBN 978-3-8348-0699-4.

[8] P. Philips, A. Schamel, J. Meyer, ”An Efficient Model for Valve Train and Spring Dynamics”, in ”SAE Technical Paper 890619”, 1989.

[9] A. Schamel, J. Hammacher, D. Utsch, ”Modeling and Measurement Techniques for Valve Spring Dynamics in High Revving Internal Combustion Engines”, in ”Design of Racing and High Performance Engines”,p. 83-99, 1993.

[10] T. Engelhardt, ”Dynamik von Steuer- und Ventiltrieben”, Dissertation, Technische Universität München, 2007.

[11] R. Tichanek, D. Fremut, R. Cihak, ”The Over-Head Cam (OHC) Valve Train Computer Model”.

[12] R. Huber, J. Clauberg, H. Ulbrich ”An Efficient Spring Model Based on a Curved Beam with Non-Smooth Contact Mechanics for Valve Train Simulations”, in ”SAE World Congress 2010”, Detroit, USA, 2010.

[13] M. Schneider, K. Krüger, M. Friedrich and H. Ulbrich, ”Experiments and Simulation of Hydraulic Cam Phasing Systems”, SAE World Congress 2008 - Variable Valve Optimization, Detroit, 2008

[14] M. Förg et. al., ”Contacts within Valve Train Simulations: a Comparison of Models”, JSME Technical Journal, 1(1), 2006.